Electrostatics of ions inside the nanopores and trans-membrane channels

Y. Levin(*)

Instituto de Física, Universidade Federal do Rio Grande do Sul
Caixa Postal 15051, CEP 91501-970, Porto Alegre, RS, Brazil

Abstract. – A model of a finite cylindrical ion channel through a phospholipid membrane of width L separating two electrolyte reservoirs is studied. Analytical solution of the Poisson equation is obtained for an arbitrary distribution of ions inside the trans-membrane pore. The solution is asymptotically exact in the limit of large ionic strength of electrolyte on the two sides of membrane. However, even for physiological concentrations of electrolyte, the electrostatic barrier sizes found using the theory are in excellent agreement with the numerical solution of the Poisson equation. The analytical solution is used to calculate the electrostatic potential energy profiles for pores containing charged protein residues. Availability of a semi-exact interionic potential should greatly facilitate the study of ionic transport through nanopores and ion channels.

Ion channels are water-filled holes which facilitate exchange of electrolyte between the exterior and interior of a cell. Pores are formed by specific proteins embedded into the phospholipid membrane [1]. Depending on the conformation of the protein, the pore can be open or closed. When open, the protein is very specific to the kind of ions that it allows to pass through the channel [2,3]. In order to function properly the channel has to conduct thousands of ions in a period of few milliseconds. Considering that the channel passes through a phospholipid membrane which has a very low dielectric constant and is very narrow, producing high energetic penalties for ions entering the nonopores, it is fascinating to contemplate how Natures manages to perform this amazing task. In fact, as long ago as 1969, Parsegian observed that for an infinitely long cylindrical channel [4] of radius $a = 3\,\text{Å}$, the electrostatic barrier is over $16k_BT$, which should completely suppress any ionic flow [5]. Later numerical work by Levitt [6], Jordan [7] and others demonstrated that for more realistic finite channels the barrier is dramatically reduced. For example, for a channel of length $L = 25\,\text{Å}$ and radius $a = 3\,\text{Å}$, the barrier is about $6k_BT$, which although still quite large, should allow ionic conductivity. Recently the study of ion channels has expanded to other parts of applied physics. Water-filled nanopores are introduced into silicon oxide films, polymer membranes, etc. [8,9]. In all of these cases the dielectric constant of the interior of a nanopore greatly exceeds that of the surrounding media.

To quantitatively study the conductance of a nanopore one has three options: the all-atom molecular-dynamics simulation (MD) [3]; the Brownian-dynamics simulation (BD) [10,11] with

implicit water treated as a uniform dielectric continuum; or the mean-field Poisson-Nernst-Planck theory (PNP) [12], which treats both water and ions implicitly. While clearly the most accurate, MD simulations are computationally very expensive [13]. Brownian dynamics is significantly faster than MD, but because of the dielectric discontinuities across the various interfaces a new solution of the Poisson equation is required for each new configuration of ions inside the pore. The simplest approach to study the ionic conduction is based on the PNP theory [12]. This combines the continuity equation with the Poisson equation and Ohm's and Fick's laws. PNP is intrinsically mean-field and is, therefore, bound to fail when ionic correlations become important. This has been well studied for its static version — the Poisson-Boltzmann equation, which is known to break down for aqueous electrolytes with multivalent ions and also for monovalent electrolytes in low dielectric solvents [14, 15]. For narrow channels, the cylindrical geometry, combined with the field confinement, results in a pseudo–one-dimensional potential of very long range [16, 17]. Under these conditions the correlational effects dominate, and the mean-field approximation fails [14]. Indeed recent comparison between the BD and the PNP showed that PNP breaks down when the pore radius is smaller than about two Debye lengths [10, 11]. At the moment, therefore, it appears that a semi-continuum (implicit solvent) Brownian-dynamics simulation is the best compromise between the cost and accuracy [13, 18, 19] for narrow pores. Unfortunately even this, simplified strategy demands a tremendous computational effort. The difficulty is that BD requires a new solution of the Poisson partial differential equation at each time step. This can be partially overcome by using lookup tables [11] and variational methods [20], but still requires a supercomputer. If the interaction potential between the ions inside the channel were known, the simulation could proceed orders of magnitude faster. However, up to now the only exact solution to the Poisson equation in a cylindrical geometry was for the case of an infinitely long pore [4, 5, 16]. In this letter we shall provide another exact solution, but now for a finite trans-membrane channel.

We shall work in the context of a primitive model of electrolyte and membrane. The membrane will be modeled as a uniform dielectric slab of width L located between $z = 0$ and $z = L$. The dielectric constant of the membrane and the channel forming protein is taken to be $\epsilon_p \approx 2$. On both sides of the membrane there is an electrolyte solution composed of point-like ions and characterized by the inverse Debye length κ. A channel is a cylindrical hole of radius a and length L filled with water. As is usual for continuum electrostatic models [13], we shall take the dielectric constant of water inside and outside the channel to be the same, $\epsilon_w \approx 80$. It is convenient to set up a cylindrical coordinate system (z, ρ, ϕ) with the origin located on the symmetry axis of the channel at $z = 0$. Suppose that an ion is located at an arbitrary position $\boldsymbol{x}'$ inside the channel. The electrostatic potential $\varphi(z, \rho, \phi; \boldsymbol{x}')$ inside the channel and membrane satisfies the Laplace equation

$$\nabla^2 \varphi = -\frac{4\pi q}{\epsilon_w} \delta(\boldsymbol{x} - \boldsymbol{x}') \ . \tag{1}$$

For $z > L$ and $z < 0$, $\varphi(\boldsymbol{x}; \boldsymbol{x}')$ satisfies the linearized Poisson-Boltzmann or the Debye-Hückel equation [14]

$$\nabla^2 \varphi = \kappa^2 \varphi \ . \tag{2}$$

The inverse Debye length is related to the ionic strength I of electrolyte, $\xi_D^{-1} = \kappa = \sqrt{8\pi \lambda_B I}$, where $\lambda_B = q^2/\epsilon k_B T$ is the Bjerrum length and $I = (\alpha^2 c_\alpha + \alpha c_\alpha + 2c)/2$. Here c_α is the concentration of $\alpha : 1$ valent electrolyte and c is the concentration of $1 : 1$ electrolyte. All the usual boundary conditions must be enforced: the potential must vanish at infinity and be continuous across all the interfaces; the tangential component of the electric field and the normal component of the electric displacement must be continuous across all the interfaces.

These boundary conditions guaranty the uniqueness of solution. Unfortunately, even this relatively simple geometry cannot, in general, be solved exactly. We observe, however, that an *exact* solution is possible in the limit that $\kappa \to \infty$. In this special case the system of differential equations becomes separable. Our, strategy then will be to solve exactly this asymptomatic problem and then extend the solution to finite values of Debye length.

We start by making the following fundamental observation. The condition $\kappa \to \infty$ signifies that electrolyte perfectly screens any electric field —the Debye length is zero. This, combined with the boundary condition —electrostatic potential must vanish at infinity— implies that in this limit $\varphi(0, \rho, \phi; \boldsymbol{x}') = \varphi(L, \rho, \phi; \boldsymbol{x}') = 0$, for *any* position $\boldsymbol{x}'$ of an ion inside the pore. This is a dramatic simplification. Now it is no longer necessary to solve the Debye-Hückel equation, but only the Poisson equation with a perfect grounded conductor boundary conditions at $z = 0$ and $z = L$. To proceed we expand the $\delta(z - z')$ in eigenfunctions of the differential operator

$$\frac{\mathrm{d}^2 \psi_n}{\mathrm{d}z^2} + k_n^2 \psi_n = 0 \, , \tag{3}$$

satisfying the perfect-conductor boundary condition. The normalized eigenfunctions are $\psi_n(z) = \sqrt{2/L} \sin(k_n z)$, with $k_n = n\pi/L$. The Sturm-Liouville nature of the differential equation (3) guarantees us that

$$\delta(z - z') = \frac{2}{L} \sum_{n=1}^{\infty} \sin(k_n z) \sin(k_n z') \, . \tag{4}$$

Similarly,

$$\delta(\phi - \phi') = \frac{1}{2\pi} \sum_{m=-\infty}^{\infty} e^{im(\phi - \phi')} \, . \tag{5}$$

Next we write

$$\varphi(\boldsymbol{x}, \boldsymbol{x}') = \frac{q}{\pi \epsilon_w L} \sum_{n=1}^{\infty} \sum_{m=-\infty}^{\infty} e^{im(\phi - \phi')} \sin(k_n z) \sin(k_n z') g_{nm}(\rho, \rho') \, . \tag{6}$$

Substituting this into eq. (1) we find that the Green function $g_{nm}(\rho, \rho')$ satisfies the modified Bessel equation

$$\frac{1}{\rho} \frac{\mathrm{d}}{\mathrm{d}\rho} \rho \frac{\mathrm{d}g_{nm}}{\mathrm{d}\rho} - \left(k_n^2 + \frac{m^2}{\rho^2} \right) g_{nm} = -\frac{4\pi}{\rho} \delta(\rho - \rho'), \tag{7}$$

the solution of which can be found using the usual techniques [4, 21]. We obtain

$$g_{mn}(\rho, \rho') = 4\pi I_m(k_n \rho_<)[K_m(k_n \rho_>) + \gamma_{mn} I_m(k_n \rho_>)], \tag{8}$$

where $\rho_>$ and $\rho_<$ are the larger and the smaller of the set (ρ, ρ') and

$$\gamma_{mn} = \frac{K_m(k_n a) K'_m(k_n a)(\epsilon_p - \epsilon_w)}{\epsilon_w I'_m(k_n a) K_m(k_n a) - \epsilon_p I_m(k_n a) K'_m(k_n a)} \, . \tag{9}$$

Here I_m, K_m, I'_m, K'_m are the modified Bessel functions of the first and second kind and their derivatives, respectively. Equation (8) is valid for $\rho_> \leq a$. When $\rho > a$,

$$g_{mn}(\rho, \rho') = \frac{4\pi \epsilon_w}{k_n a} \frac{K_m(k_n \rho) I_m(k_n \rho')}{\epsilon_w I'_m(k_n a) K_m(k_n a) - \epsilon_p I_m(k_n a) K'_m(k_n a)} \, . \tag{10}$$

Equations (6), (8), and (10) are exact for an ion inside a pore with perfect-conductor boundary conditions at $z = 0$ and $z = L$. If the ion is located on the axis of symmetry, $z' = z_0$, $\rho' = 0$,

only the $m = 0$ term in eq. (6) survives, and the electrostatic potential *inside* the channel at position z, ρ takes a particularly simple form, $\varphi_{in}(z, \rho; z_0) = \varphi_1(z, \rho; z_0) + \varphi_2(z, \rho; z_0)$, where

$$\varphi_1(z, \rho; z_0) = \frac{4q}{\epsilon_w L} \sum_{n=1}^{\infty} \sin(k_n z) \sin(k_n z_0) K_0(k_n \rho) , \tag{11}$$

and

$$\varphi_2(z, \rho; z_0) = \frac{4q(\epsilon_w - \epsilon_p)}{\epsilon_w L} \sum_{n=1}^{\infty} \frac{K_0(k_n a) K_1(k_n a) I_0(k_n \rho) \sin(k_n z) \sin(k_n z_0)}{\epsilon_w I_1(k_n a) K_0(k_n a) + \epsilon_p I_0(k_n a) K_1(k_n a)} . \tag{12}$$

Equations (11), (12) are exact in the $\kappa \to \infty$ limit. To see how these equations can be extended to finite values of κ, it is important to first understand their physical meaning. Potential φ_2 is mostly the result of the charge induced on the interface between the high dielectric aqueous interior of the pore and the low dielectric membrane. We expect that this term will be affected very little by the precise value of the Debye length of the surrounding electrolyte solution.

The potential φ_1 contains the contribution from the ion located at z_0 and from the induced charge on the pore/electrolyte and the membrane/electrolyte interfaces. It will, therefore, strongly depend on the precise value of κ. Furthermore, we observe that eq. (11) is *exactly* the potential produced by a charge q located inside an *infinite* slab of water of width L bounded by two grounded perfectly conducting planes [21]. This key observation allows us to explicitly resum the series in eq. (11). However, it is possible to do even better, and now enforce the *exact* boundary condition, namely that for $z < 0$ and $z > L$ the electrostatic potential must satisfy the Debye-Hückel equation (2). Using the Bessel J representation of the delta-function one can constructs the Green function [22] which satisfies all the boundary conditions for the slab geometry and has the required symmetry property [21] between the source and the observation points. We then find

$$\varphi_1(z, \rho; z_0) =$$
$$\int_0^{\infty} dk \frac{J_0(k\rho) \left\{ \alpha^2(k) e^{k|z-z_0|-2kL} + \alpha(k)\beta(k)[e^{-k(z+z_0)} + e^{k(z+z_0)-2kL}] + \beta^2(k) e^{-k|z-z_0|} \right\}}{\beta^2(k) - \alpha^2(k) \exp[-2kL]} , \tag{13}$$

where $\alpha(k) = [k - \sqrt{k^2 + \kappa^2}]/2k$, $\beta(k) = [k + \sqrt{k^2 + \kappa^2}]/2k$, and $J_0(x)$ is the Bessel function of first kind and order zero. Equation (13) provides an analytic continuation of eq. (11) into finite κ parameter space. It can be checked explicitly that in the limit $\kappa \to \infty$, eq. (13) exactly sums the series in eq. (11). Finally, for the region $\rho > a$ the electrostatic potential is

$$\varphi_{\text{out}}(z, \rho; z_0) = \frac{4q}{L} \sum_{n=1}^{\infty} \frac{1}{k_n a} \frac{K_0(k_n \rho) \sin(k_n z) \sin(k_n z_0)}{\epsilon_w I_1(k_n a) K_0(k_n a) + \epsilon_p I_0(k_n a) K_1(k_n a)} . \tag{14}$$

Equation (14) is exact only for the perfect conductor boundary conditions, however, the huge jump in the dielectric constant going from the membrane's interior to the aqueous electrolyte will leave φ_{out} mostly unaffected even for finite values of κ.

If the channel contains N ions and charged protein residues their interaction energy is given by

$$V = \frac{1}{2} \sum_{i,j}^{N} q_i \varphi^j , \tag{15}$$

where q_i is the charge of ion/residue i and φ^j is the electrostatic potential produced by the ion/residue j at the position of ion/residue i. Similarly the electrostatic barrier that an ion feels as it moves through a charge free channel is [14],

$$U(z) = \frac{q}{2} \lim_{\rho \to 0} \left[\varphi(z, \rho; z) - \frac{q}{\epsilon_w \rho} \right] + \frac{q\kappa}{2\epsilon_w} . \tag{16}$$
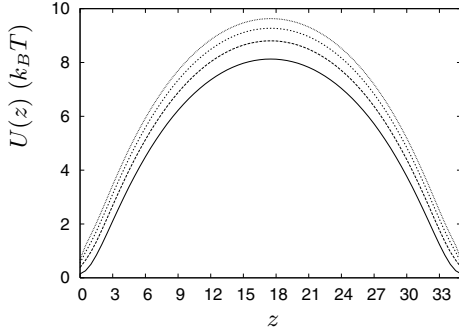
Fig. 1

Fig. 2

Fig. 1 – Electrostatic potential barriers for an ion of charge q moving along the axis of symmetry through a channel of $L = 35\,\text{Å}$ and $a = 3\,\text{Å}$. External electrolyte concentration from bottom to top is 0.15, 1, 2 and 3 M.
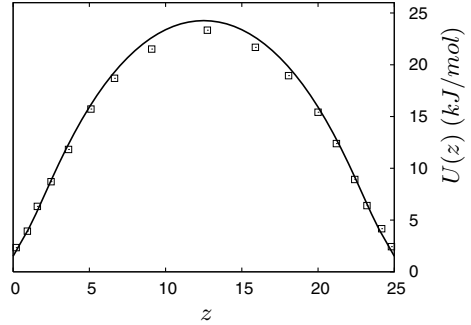
Fig. 2 – Electrostatic potential barrier for an ion of charge q moving through a pore of $L = 25\,\text{Å}$ and $a = 2.5\,\text{Å}$. External electrolyte concentration is 2.5 M. Symbols are the result of a numerical integration of the system of Poisson-Boltzmann (bulk electrolyte) and Poisson equation (pore interior) from ref. [23].

The last term in eq. (16) is the electrostatic "solvation" energy that a point-like ion loses as it moves from the bulk electrolyte into the interior or a pore. This energy can be calculated using the Debye-Hückel theory and is equivalent to the excess chemical potential resulting from the screening of ionic electric field by the surrounding electrolyte [14]. The limit in eq. (16) is easily obtained by noting that

$$\frac{1}{\rho} = \int_0^\infty J_0(k\rho)\mathrm{d}k \ . \tag{17}$$

We are now in a position to explore some of the quantitative consequences of the current theory. In fig. 1 we first plot the potential energy barrier for an ion of charge q moving through a channel of $L = 35\,\text{Å}$ and $a = 3\,\text{Å}$ and various external electrolyte concentrations. For the physiological salt concentration (150 mM) we find the barrier height to be $8.13k_BT$. Using numerical solution of the Poisson equation, Levitt obtained a barrier of $8.48k_BT$. Some of the difference between the two values can be attributed to the fact that in numerical calculations presence of external electrolyte was not taken into account. As the length of the channel increases, the role of external electrolyte becomes relatively less important. Indeed for a channel of $L = 50\,\text{Å}$ and $a = 2\,\text{Å}$, we obtain a barrier of $18.65k_BT$, while the Levitt's numerical solution produced $17.2k_BT$ [6] and Jordan's $18.6k_BT$ [7]. The only numerical work known to us that explicitly takes into account the existence of the external electrolyte is ref. [23]. The authors of that paper numerically solved the non-linear Poisson-Boltzmann equation for the external electrolyte and the Poisson equation for the interior of the channel. For a pore of $L = 25$ and $a = 2.5\,\text{Å}$, and electrolyte concentration of 2.5 M, they find a barrier of $9.5k_BT$, while we obtain $9.8k_BT$. In fig. 2 we compare the full electrostatic energy barrier obtained from the numerical solution with our analytical results. The agreement, once again, is quite good.

Availability of a semi-exact interaction potential allows us to easily explore the potential energy landscape $\Phi = V + U$ of an ion of charge q moving through a channel which also contains some fixed charged protein residues. For example, consider a channel of $L = 35\,\text{Å}$ and $a = 3\,\text{Å}$ and suppose that there is one protein residues of charge $-q$, embedded into the surface of the channel at $(z = L/2, \rho = a, \phi)$. In fig. 3 we show the potential energy profile for an ion
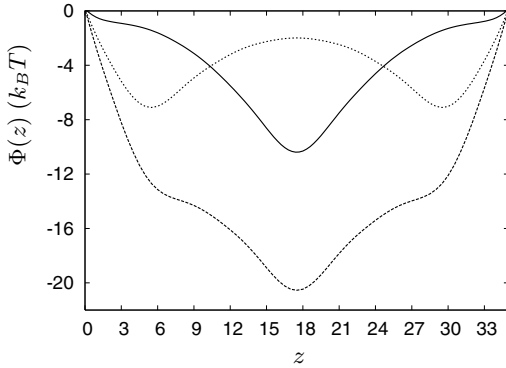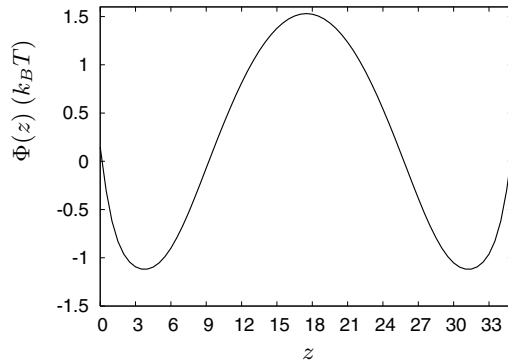
Fig. 3

Fig. 4

Fig. 3 – Potential energy profile for an ion of charge q moving along the axis of symmetry through a channel of $L = 35\,\text{Å}$ and $a = 3\,\text{Å}$ containing a protein residue of charge $-q$ embedded into its wall ($\rho = a$) at $z = L/2$ (solid line); containing two charged residues at $z = 5$ and $z = 30\,\text{Å}$ (dotted line); containing three residues at $z = 5, 17.5$ and $z = 30\,\text{Å}$ (dashed line). External electrolyte concentration is $150\,\text{mM}$.

Fig. 4 – Potential energy profile for an ion of charge q moving along the axis of symmetry through a pore of $L = 35\,\text{Å}$ and $a = 3\,\text{Å}$, containing two charged residues hidden in the membrane's interior ($\rho = 6\,\text{Å}$) located at $z = 5$ and $z = 30\,\text{Å}$. External electrolyte concentration $150\,\text{mM}$.

moving along the axis of symmetry through such a channel. Instead of a potential barrier, this ion encounters a potential well of depth more than $10k_BT$! It will, therefore, find it extremely difficult to pass through such a channel.

Now, suppose that two charged residues are embedded into the channel wall, one close to the entrance of the channel at $z = 5\,\text{Å}$ and another close to its exit at $z = 30\,\text{Å}$, both at $\rho = 3\,\text{Å}$. The electrostatic potential, now develops a double-well structure, fig. 3. Each minimum is relatively less deep than in a channel with only one central residue. One might then suppose that adding more charged residues will diminish the depth of the wells even further. This, however, is not the case. In fig. 3 we also show the potential-energy landscape of a channel containing three uniformly spaced residues. Evidently instead of decreasing the depth of the potential well, it has dramatically increased! There is, however, a mechanism which Nature can use to diminish the depth of potential wells —hide the charged residues in the membrane's (or protein's) hydrophobic interior [24]. In fig. 4 we plot the potential energy profile for the same channel as in fig. 3, but with the two charged residues hidden in the membrane's hydrophobic interior at $\rho = 6\,\text{Å}$. In this case the deep potential well is replaced by a shallow binding site followed by an activation barrier of only $2.5k_BT$. This can be easily overcome by an external electric field or a chemical potential gradient. We find that there is an optimum location for hiding charged residues in order to produce the smallest barrier for channel penetration. The formalism developed above allows us to easily explore all the parameter space in order to find this optimum position.

To conclude, we have presented an analytically solvable model of electrostatics inside an ion channel. The solution found is exact in the limit of large electrolyte concentrations. However, comparison with the numerical work shows that it remains valid even at intermediate and low electrolyte concentrations. The analytical solution can be used to dramatically speed up the Brownian-dynamics simulations of ionic transport through cylindrical pores. The biological and structural information can be partially taken into account through a proper placement of

charged protein residues. Furthermore, even if a more detailed atomistic molecular-dynamics simulation is necessary, availability of a rapid Brownian-dynamics model can serve for a initial exploration of the parameter space.

In this work water inside the pore has been treated as a uniform dielectric continuum identical to the bulk. While this is acceptable for wider pores, the approximation will certainly fail for very narrow pores such as gramicidin. To properly account for the polarization of water in this geometry, one must go beyond the continuum dielectric approximation [25]. Until now, the only option for these cases was to perform all-atom molecular-dynamics simulations. The current work suggests that another way might be possible. The continuum description with $\epsilon_w = 80$ and $\epsilon_p = 2$ can be used for the bulk water outside the channel, for the membrane, and for the trans-membrane protein, while inside the channel (now with $\epsilon_{in} = 1$) one might try to obtain an accurate analytical electrostatic potential. The Coulomb interactions between the water molecules inside the channel could then be treated explicitly, without any need for continuum dielectric approximation. This would then allow to perform very fast molecular-dynamics simulations of ionic transport, free of the drawbacks associated with the implicit solvent models. The work in this direction is now in progress.

$$* * *$$

REFERENCES

[1] HILLE B., *Ionic Channels of Excitable Membranes*, 3rd edition (Sinauer Associates, Sunderland, MA) 2001.
[2] DOYLE D. A. *et al.*, *Nature*, **280** (1998) 69.
[3] ROUX B. and BERNECHE S., *Nature*, **414** (2001) 73.
[4] SMYTHE W. R., *Static and Dynamic Electricity* (McGraw-Hill, New York) 1950.
[5] PARSEGIAN A., *Nature*, **221** (1969) 844.
[6] LEVITT D. G., *Biophys. J.*, **22** (1978) 209.
[7] JORDAN P. C., *Biophys. J.*, **39** (1982) 157.
[8] LI J. *et al.*, *Nature*, **412** (2001) 166.
[9] SIWY Z. and FULINSKI A., *Phys. Rev. Lett.*, **89** (2002) 198103.
[10] MOY G., CORRY B., KUYUCAK S. and CHUNG S. H., *Biophys. J.*, **78** (2000) 2349.
[11] CORRY B., KUYUCAK S. and CHUNG S. H., *Biophys. J.*, **78** (2000) 2364.
[12] EISENBERG R. S., *J. Membr. Biol.*, **171** (1999) 1.
[13] LEVITT D. G., *J. Gen. Physiol.*, **113** (1999) 789.
[14] LEVIN Y., *Rep. Prog. Phys.*, **65** (2002) 1577.
[15] NAJI A., JUNGBLUT S., MOREIRA A. G. and NETZ R. R., *Physica A*, **352** (2005) 131.
[16] TEBER S., *J. Stat. Mech. Theory Exp.* (2005) P07001.
[17] ZHANG J., KAMENEV A. and SHKLOVKSII B. I., *Phys. Rev. Lett.*, **95** (2005) 148101.
[18] KUYUCAK S., ANDERSEN O. S. and CHUNG S. H., *Rep. Prog. Phys.*, **64** (2001) 1427.
[19] TIELEMAN D. P., BIGGIN P. C., SMITH G. R. and SANSOM M. S. P., *Q. Rev. Biophys.*, **34** (2001) 473.
[20] ALLEN R., MELCHIONNA S. and HANSEN J. P., *Phys. Rev. Lett.* (2002) 175502.
[21] JACKSON J. D., *Classical Electrodynamics* (Wiley, New York) 1999.
[22] LEVIN Y. and FLORES-MENA J. E., *Europhys. Lett.*, **56** (2001) 187.
[23] JORDAN P. C., BACQUET R. J., MCCAMMON J. A. and TRAN P., *Biophys. J.*, **55** (1989) 1041.
[24] KUYUCAK S. and BASTUG T., *J. Biol. Phys.*, **29** (2003) 429.
[25] PETER C. and HUMMER G., *Biophys. J.*, **89** (2005) 2222.